Journal of the Brazilian Society of Mechanical Sciences and Engineering (2020) 42:501
https://doi.org/10.1007/s40430-020-02580-3

TECHNICAL PAPER

Design and control of spatial inverted pendulum with two degrees of freedom

Atilla Bayram[1] · **Firat Kara**[2]

Received: 30 November 2019 / Accepted: 19 August 2020 / Published online: 8 September 2020

Abstract
The inverted pendulum systems have inherently unstable dynamics. In order to stabilize the inverted pendulum at upright position, an actuation mechanism should generate fast-reactive motions at the pivot point of the system. This paper addressed the design and control of a spatial inverted pendulum with two degrees of freedom (DOF). The first part of the study consists of designing a novel planar two-DOF (PRRRR) actuation mechanism in order to balance the spatial inverted pendulum. The system is underactuated and has inherently extreme nonlinearity and also the restrictions on the actuators. Then, in the second part, a second-order sliding-mode and a linear quadratic Gaussian (LQG) controller have been proposed to control the pendulum within the equilibrium position. Finally the simulation results evaluated in terms of the robustness, time response and stability show that the second-order sliding-mode controller is more robust and has fast response performances in re-stabilizing the spatial inverted pendulum, while LQG controller is better in terms of keeping the system in equilibrium during the long period of time.

Keywords Two degrees of freedom inverted pendulum · Spatial inverted pendulum · Sliding-mode control · Linear quadratic Gaussian

1 Introduction

In order to balance a stick on the fingertip or palm of the hand, the pose of the pivoting point needs to be rapidly moved along its falling direction. The inverted pendulum problem is based on the same principle. Just like the stick, the inverted pendulum system has the same inherently unstable dynamics. Due to their nonlinear models, need of quick response, and unstable behaviors, the inverted pendulum-based systems have served the researchers in the control field as a subtle control problem for a long time. To realize experimental models, to verify new control techniques, to improve existing control methods, and especially to represent real engineering applications, the inverted pendulum systems have become one of the main focuses for the researchers. Nonlinear inverted pendulum dynamics are utilized in some specific subjects such as modeling of human posture and gait [1], control of robotic arms used in pick and place operations [2], flight controls of rocket and missiles [3], balancing the landing modules of airplanes and helicopter and air vehicles in turbulence [4], etc.

The literature contains a very large family of inverted pendulum systems with many different configurations. Most of them are a single inverted pendulum actuated with a linear car or skidder moving in one direction [5]. Also, there are some studies based on double inverted pendulum balanced using again a single actuator [6, 7]. The common point of these inverted pendulum systems mentioned above is that the number of actuators is less than the degrees of freedom of the system. In other words, they are deficient or underactuated [8].

The other inverted pendulum group, which is also the subject of this paper, is the spatial inverted pendulums with two degrees of freedom. Unlike many studies [9, 10] in which the rotational axes are parallel to each other and the rotational motion occurs on a single plane, the spatial inverted pendulum is designed so that two rotational axes

Technical Editor: Victor Juliano De Negri, D.Eng.

✉ Atilla Bayram
atillabayram@yyu.edu.tr

[1] Mechanical Engineering Department, Faculty of Engineering, VAN Yuzuncu Yil University, Van, Turkey

[2] Mechanical Engineering, Faculty of Engineering, İzmir Institute of Technology, İzmir, Turkey

are orthogonal to each other and the pendulum is prevented from rotating around its own axis and can easily tilt over any direction in 3D space. Spatial inverted pendulum systems are classified in three basic groups depending on the mechanism used to stabilize the pendulum [11]. The studies of Soto [12] and Ishii [11] can also be added in these three categories as a fourth type. The first type among this classification is a system where a spatial inverted pendulum connected to the *X*–*Y* table is controlled by applying linear motions in *x* and *y* directions in horizontal plane parallel to the ground [13]. The spatial inverted pendulum systems mounted on a multi-directional vehicle can be mentioned as the second type. In these systems, unlike the *X*–*Y* table, the same planar motion is obtained by using wheels that can move in more than one direction. Another difference from the *X*–*Y* table systems is that the pendulum can turn around its own axis [14, 15]. In the third type, robotic arms with serial configurations are used to balance a spatial pendulum [16, 17]. In the fourth type, a spatial inverted pendulum is mounted on a five-bar planar mechanism highly studied in the literature. In these systems, the pendulum is controlled by the motion generated through a mechanism with two rotational inputs [11, 12].

As known, control methods are generally divided into model-dependent and model-free methods. In cases, where the dynamic model represents the system strongly, the methods such as sliding-mode control, model predictive control and computational torque control are used, whereas the model-free methods like artificial neural networks, fuzzy logic and standard PID methods are used to control the system where the model cannot be obtained precisely. Besides, in the literature, the PID methods are also used on model-based controllers such as the model based PID controller with Ziegler–Nichols tuning. In the studies carried out on four different types of spatial inverted pendulum mentioned previously, the controllers have been designed based on the model-free or linearized model. A PID controller was successfully applied on the *X*–*Y* table pendulum system [13]. In addition, on a very similar system, there are also some studies using sliding-mode control [18], artificial neural networks, fuzzy neural networks [19] and adaptive sliding-mode control [20]. In another study, the spatial inverted pendulum was stabilized at the unstable upright position by using the adaptive feedback controller designed with the help of the Lyapunov function [12]. Furthermore, other studies using similar setups have accomplished the stabilization via the controllers of fuzzy logic [21] and linear quadratic regulators [22]. In third type of the inverted pendulum system, the control operation was executed through a three-DOF robot arm. In this study, the controller involved two linear and one nonlinear controller based on energy and kinetic momentum [16]. In another energy based method, a feedback control method using Tereshko [23] by altering the energy of the chaotic system was presented to control an inverted pendulum with parametric errors [24]. This method converts the chaotic behavior of the pendulum into a periodic oscillation.

In control of spatial case, a spatial inverse pendulum was compensated by a serial robot arm with three DOF but planar motion. The dynamic equations were linearized to design the linear quadratic regulator (LQR) controller. There are only a few studies in literature on the spatial inverted pendulum actuated five bar mechanism. The researchers designed the controllers for the stabilization of the pendulum based on H_∞ robust control method and the linear quadratic regulator over the linearized model respectively [11, 12].

In this paper, a spatial inverted pendulum was stabilized by using a novel two-DOF PRRRR (P: Prismatic joint, R: Revolute joint) planar mechanism driven with one rotational and one linear actuators. The tangible contribution of the study is the balancing an inverted pendulum by means of a novel actuation mechanism. Therefore, this mechanism presented in this paper can be regarded as the fifth type of mechanism in balancing of spatial pendulums. The reason why this mechanism is preferred is that first it can create higher accelerations at the pivot point where the spatial pendulum is mounted to the mechanism. Secondly, the nonlinear model of the pendulum system with the joint limitation has revealed an opportunity with a very complex structure to assess the performance of control methods. This study involves design of a planar PRRRR mechanism to generate the required forces to keep the spatial pendulum at equilibrium position. This design procedure is to determine the dimensions of the mechanism maximizing the workspace by using the kinematic analysis and the genetic algorithm (GA). In the second stage, the studies were implemented on the control of the inverted pendulum. Finally, the spatial inverted pendulum system was simulated by using a nonlinear method of the second-order sliding-mode control (SOSMC) and also the linear quadratic Gaussian (LQG) method through the linearization of the dynamic model. At the end of this study, the two control methods were evaluated comparatively according to performance criteria such as fast response, stability and robustness for the disturbances.

2 The modeling of inverted spatial pendulum system

This section addresses the construct and kinematic analysis of the PRRRR actuation mechanism and the dimensional optimization with genetic algorithm. Then, the dynamic analysis of the whole spatial inverted pendulum system and the controller design which holds the pendulum in equilibrium points will be emphasized. Here, all the joints, links and pendulum were assumed to be rigid. Figure 1 shows the CAD model of the spatial inverted pendulum and its

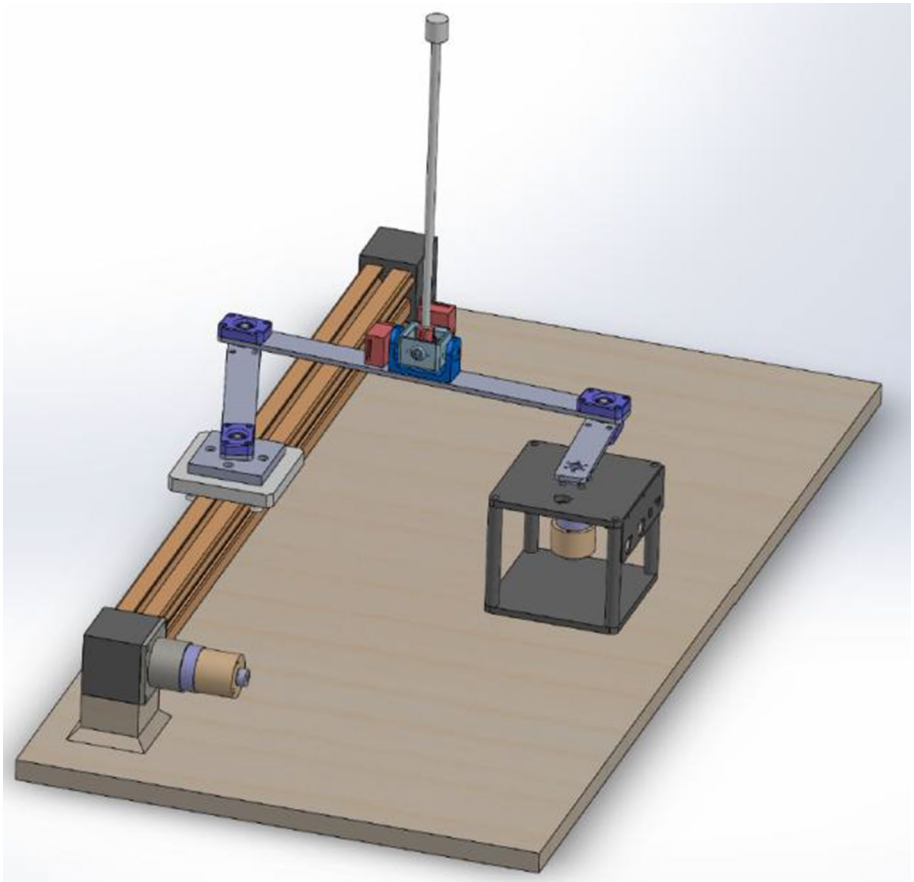

Fig. 1 The CAD model of the spatial inverted pendulum system

actuation mechanism presented in this paper. This system possesses a total of 4 DOFs, two from the PRRRR mechanism and two from the spatial inverted pendulum. The pendulum has two rotational DOFs whereas the actuation mechanism has two positional DOFs for the associated pivot point. This system does not allow the self-swing control since the space which is pendulum works is limited.

The actuation mechanism has a planar structure and its four links are connected with one prismatic (P) and four revolute (RRRR) joints (Fig. 2). The first input applied to the system is a linear actuator represented by the prismatic joint, which can be driven by means of a linear gantry. For the second input, the revolute joint at the other end of the mechanism was selected as a rotational actuator. In this case, the P and R actuated joints represented by s_5 and θ_2

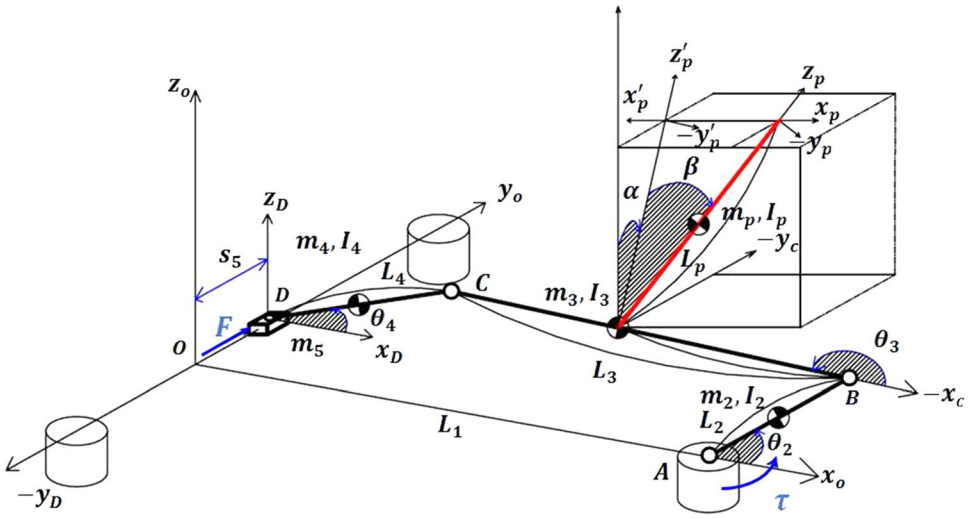

Fig. 2 The schematic diagram of the PRRRR mechanism and spatial inverted pendulum system

are active while the other two revolute joints represented by θ_3 and θ_4 are passive. The spatial inverted pendulum is connected to the actuation mechanism via a universal joint with two DOFs. Thus, this pendulum can be tilted freely from the upright position to the horizontal motion plane of the mechanism.

The spatial inverted pendulum becomes unstable by deviating from the equilibrium positions. This may be caused by the disturbing effects from the environment and/or the system itself and unbalanced inertial effects as well. For this reason, the dynamic balancing forces with the varying directions and magnitudes should be produced to keep the system in equilibrium or to compensate it again. These dynamic forces created by the actuation mechanism must fulfill the stabilization by repositioning the pivot point (O_j) which connects the pendulum to the lower platform.

2.1 The kinematic analysis of the actuation mechanism

In order to produce the compensating forces properly, the pivot point (O_j) where the pendulum is connected to the mechanism must move around as wide as possible within the workspace. In addition, there must be no any restrictions on the actuators especially on the rotational one, in other words, the active joints should be capable of continuous motion for all over the operations. For this reason, finding relatively the largest and most dexterous workspace is of great importance for the design of actuation mechanism. There are various classifications on workspace of the mechanisms in literature, such as reachable or Cartesian workspace, dexterous workspace, orientation workspace, etc. In this study, the focus will be on the most dexterous workspace of the mechanism to avoid the joint restrictions in stabilizing the spatial inverted pendulum.

According to Fig. 2 , the mechanism has only one closed loop and the vectorial equation, $\left|\overrightarrow{OA}\right| + \left|\overrightarrow{AB}\right| + \left|\overrightarrow{BC}\right| = \left|\overrightarrow{OD}\right| + \left|\overrightarrow{DC}\right|$, can be written as scalar form as follows.

$$L_1 + L_2\cos\theta_2 + L_3\cos\theta_3 = L_4\cos\theta_4 \tag{1}$$

$$L_2\sin\theta_2 + L_3\sin\theta_3 - s_5 = L_4\sin\theta_4 \tag{2}$$

Using (1) and (2), θ_3 and θ_4 , which are passive joint variables, are carried out analytically in terms of the active joint variables, θ_2 and s_5. After defining the passive joint variables, the x and y coordinates of the pivot point O_j based on the active joint variables will be as follows.

$$x_{O_j} = L_1 + L_2\cos\theta_2 + \frac{L_3}{2}\cos\theta_3 \tag{3}$$

$$y_{O_j} = L_2\sin\theta_2 + \frac{L_3}{2}\sin\theta_2 \tag{4}$$

This pivot point will be used in the workspace analysis of the mechanism.

2.2 The dimension synthesis via genetic algorithm

As previously mentioned, in order for the spatial inverted pendulum to be kept in the upright state properly, the pendulum platform point (O_j) must have the ability to move continuously in a homogeneous workspace without singular positions. The workspace of the planar mechanism (Cartesian workspace) and the mobility of the joints on the mechanism (joint workspace) are directly related to the relative dimensions of the links of the mechanism. For this reason, an optimization study has been carried out in order to make this workspace relatively larger and to find suitable link dimensions for higher mobility. In this study, genetic algorithm has been chosen as the optimization technique in a simple way without the need for a deep search space. The genetic algorithm can be used for difficult problems that cannot be easily solved by traditional optimization methods.

The optimization was initiated primarily by the representation of dimensional parameters. A total of four-dimensional parameters, L_1, L_2, L_3 and L_4 were represented by a 1×32 population consisting of 8-bit (binary code) chromosomes. Due to the nature of the genetic algorithm, the results have been searched over the certain boundary values like $[L_{1\min} \le L_1 \le L_{1\max}, L_{2\min} \le L_2 \le L_{2\max}, L_{3\min} \le L_3 \le L_{3\max}$ and $L_{4\min} \le L_4 \le L_{4\max}$. For a finite number of the inputs of the mechanism, a fitness function given in (5) was established on the existence of the inverse kinematics of the mechanism and Jacobian-based condition index.

$$\text{Fitness Function} = f(L_i) = \frac{T + W \times \eta}{\left|(L_3/2) - L_2\right| + 1} \tag{5}$$

T is the number of the platform points, O_j falling into a prescribed region within the reachable workspace of the mechanism. W is the weighting term and η is the sum of the Local Condition Index (LCI) over the entire workspace. The local condition index is the reciprocal of the condition number. The term in the denominator has been added to ensure the workspace to be isotropic.

where $\eta = \sum_{j=1}^{N}\sum_{i=1}^{M}\left(\frac{1}{\kappa_{ij}}\right)$, $\kappa = \|J\|\ \left\|J^{-1}\right\|$, $|.|$ denotes the Euclidean norm or 2-norm of a matrix and $\|J\| = \sqrt{\text{the maximum eigenvalue of } \left(J^T J\right)}$.

In this searching, for a finite number of inputs ($M \times N$), the valid inverse kinematics solutions for the point, O_j are placed inside the specified region, while the points with no solution are excluded from this region. Thus, the elite populations with the highest cost values were chosen at each

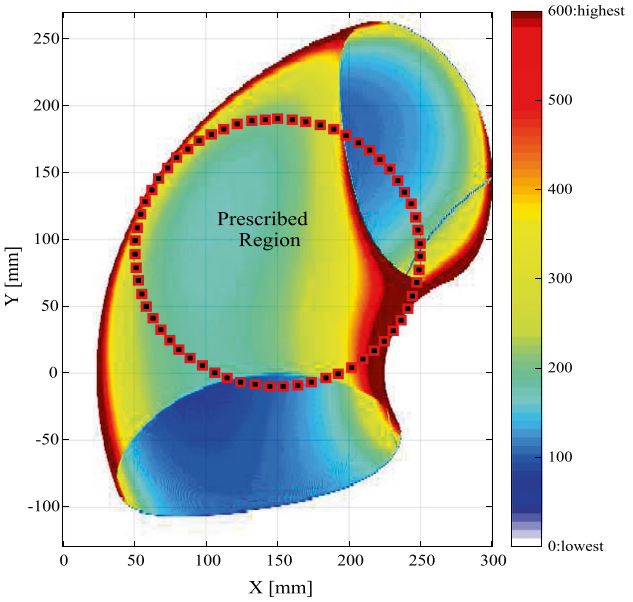

Fig. 3 The dexterous workspace of PRRRR mechanism

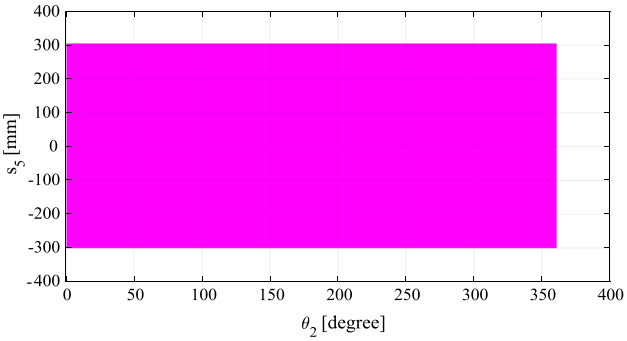

Fig. 4 The joint space of PRRRR mechanism

generation and then the best solutions were reached at the end of the optimization cycle.

As a result of the optimization performed on the range of the actuator inputs of $-300\ \text{mm} \le s_5 \le 300\ \text{mm}$ and $0° \le \theta_2 \le 360°$ with one increment, the dimension of the links shown in Fig. 2 were obtained approximately as $L_1 = 300\ \text{mm}, L_2 = 100\ \text{mm}, L_3 = 350\ \text{mm}, L_4 = 200\ \text{mm}$. Figure 3 depicts the dexterous workspace of the mechanism, which is constructed by the density of the platform points on the workspace. Meanwhile, the joint space shown in Fig. 4 is complete with these dimensions. This figure indicates that for each value of θ_2 between 0° and 360° , the mechanism can reach all values of s_5 in the range of $-300\ mm \le s_5 \le 300\ mm$ so that the inverted pendulum can move without blocking in all directions in the Cartesian workspace. If the dimensions of the mechanism were not chosen properly, serious gaps would occur within this workspace. In other words, there is no solution for the joint variables corresponding to these empty regions, i.e., the mechanism with blocking.

2.3 Dynamic analysis

Dynamic equations must be obtained for the design of model dependent controllers that are divided into two linear and nonlinear models. The equations obtained for the design of a nonlinear controller are used directly; on the other hand, the dynamic equations for linear controller design need to be linearized in the unstable upright position of the inverted pendulum. There are many methods to study the dynamic analysis of the systems in the literature, one of which is the virtual work method that eliminates the reaction forces and does not need the constraint equations too.

In this section, the dynamic equations of the spatial inverted pendulum system shown in Fig. 2 were firstly obtained by the virtual work method, and the verification of these equations was proved by the Simscape-Multibody software. The dynamic equations of the system are given as follows.

$$\sum_{i=1}^{n}[(m_i\, a_{ci} - F_i)\cdot\ \delta r_i + \left(I_i\dot{\omega}_i + \omega_i \times I_i \cdot\ \omega_i - T_i\right)\delta\varphi_i] = 0$$
$$i = 2,3,4,5,6 \tag{6}$$

where the terms of $\delta r_i = J_{V,i}\,\delta q_i$ and $\delta\varphi_i = J_{\omega,i}\,\delta q_i$ are the projections from the joint space to the task space, $J_{V,i}$ and $J_{\omega,i}$ represents the translational and rotational Jacobians respectively. In this equation, F_i $\left(T_i\right)$ involves the frictional, external, and actuation forces (torques). The statements of a_{c_i} and $\dot{\omega}_i$ denote the linear and angular accelerations of the center of gravity of each link. Since these acceleration terms include the passive joint variables, they can be written in terms of the independent joint variables as follows.

$$\left.\begin{aligned} a_{ci} &= J_{V,i}\,\ddot{q} + u_i \\ \dot{\omega}_i &= J_{\omega,i}\,\ddot{q} + w_i \end{aligned}\right\} \quad i = 2,\ 3,\ 4,\ 5, 6. \tag{7}$$

u_i and w_i contain the centrifugal and Coriolis accelerations while $q^T = [\theta_2\ \ s_5\ \ \alpha\ \ \beta]$ represents the independent joint variables. Let's substitute (7) into (6) and rearrange these equations, the dynamic equations of the spatial inverted pendulum system can be obtained in terms of the independent joint variables in a matrix form.

$$M(q)_{4\times4}\ddot{q}_{4\times4} + C(q,\dot{q})_{4\times1} = \tau_{4\times1} \tag{8}$$

$M(q)$ is a positively defined mass matrix containing the masses and inertias of the links. $C(q,\dot{q})$ is the matrix consisting of the gravity, centrifugal, Coriolis and external forces, and finally τ is the input matrix to control the system. The

equations will be used in the following sections of the study to design the controllers.

3 Controller design

In this paper, the sliding-mode control (SMC), linear quadratic regulator (LQR), and linear quadratic Gaussian (LQG) controllers will be used as controllers. They will not only try to keep the spatial inverted pendulum in an unstable equilibrium position and but also to move the pivot point through to the region where the workspace of the mechanism is highly dexterous. Thus, the mechanism will not encounter any joint restriction and will not be in the singular position during a long period of operation.

3.1 The second-order sliding-mode control (SOSMC)

Sliding-mode control (SMC) is a nonlinear control method that forces a nonlinear system to "slide" on a defined error surface by means of a discontinuous control signal. In this controller, the control law with feedback is not a continuous function of time. Instead, it is switched from a continuous structure to another one depending on the current position in the state space. In this study, the second-order sliding-mode control is proposed for the control of the spatial inverted pendulum system since it eliminates the chattering effects.

The dynamic equations must be written in the desired form so that the SMC can be designed easily. (8) must first be rearranged in the semi-open form by separated into active and passive independent variables, and then only the feedback output should be partially linearized. The linearization process is done according to the independent variables to be controlled, by arranging the equations in the different form.

If the desired outputs are also used as active independent variables (actuated independent joint variables) then the equations should be collocated and if the outputs to be controlled are passive independent variables (pendulum angles) then the equations should be written in non-collocated form [25]. In this study, since the control of active and passive variables will be performed alternately, the equations should be arranged in both types.

Let's rearrange (8) as the passive and active forms as follows.

$$\begin{bmatrix} M_{aa} & M_{ap} \\ M_{pa} & M_{pp} \end{bmatrix} \begin{bmatrix} \ddot{q}_a \\ \ddot{q}_p \end{bmatrix} + \begin{bmatrix} C_a \\ C_p \end{bmatrix} = \begin{bmatrix} \tau \\ 0 \end{bmatrix} \tag{9}$$

where $q_a = [\theta_2 \ s_5]^T$ and $q_p = [\alpha \ \beta]^T$ are active and passive joint variables respectively. Convert this matrix equation into scalar equations.The details of these coefficient matrices are given in "Appendix".

$$M_{aa}\ddot{q}_a + M_{ap}\ddot{q}_p + C_a = \tau \tag{10}$$

$$M_{pa}\ddot{q}_a + M_{pp}\ddot{q}_p + C_p = 0 \tag{11}$$

Collocated form: When $\ddot{q}_p$ is taken from (11) and then substituted into (10), the following equation involves the active joint variables, $\ddot{q}_a$.

$$\left(M_{aa} - M_{ap}{M_{pp}}^{-1}M_{pa}\right)\ddot{q}_a + \left(C_a - M_{ap}{M_{pp}}^{-1}C_p\right) = \tau \tag{12}$$

$$\bar{M}_a = M_{aa} - M_{ap}{M_{pp}}^{-1}M_{pa}$$
$$\bar{C}_a = C_a - M_{ap}{M_{pp}}^{-1}C_p$$

Substituting all these equations into (12), the control actions to be applied on the mechanism can be obtained as follows.

$$\tau = \bar{M}_a\ddot{q}_a + \bar{C}_a \tag{13}$$

Non-Collocated form: In this case, the equations are rearranged in terms of the passive joint variables of $\ddot{q}_p$ like the previous operations.

$$\left(M_{ap} - M_{aa}{M_{pa}}^{-1}M_{pp}\right)\ddot{q}_p + \left(C_a - M_{aa}{M_{pa}}^{-1}C_p\right) = \tau \tag{14}$$

$$\bar{M}_p = M_{ap} - M_{aa}{M_{pa}}^{-1}M_{pp}$$
$$\bar{C}_p = C_a - M_{aa}{M_{pa}}^{-1}C_p$$

Substituting all these equations into (14), the control actions to be applied on the mechanism depending on the passive joint variables can be obtained as follows.

$$\tau = \bar{M}_p\ddot{q}_p + \bar{C}_p \tag{15}$$

Twisting sliding-mode controller (higher-order sliding-mode controller) (TSMC) design: The controller design should be started by describing the sliding surfaces to control the pendulum angles.

$q_{rp} = [\alpha_r \beta_r]^T$: the reference pendulum angles

$q_p = [\alpha \ \beta]^T$: the instantaneous measured pendulum angles

The sliding surfaces can be written as follows.

$s = (q_{rp} - q_p)$ and $\dot{s} = (\dot{q}_{rp} - \dot{q}_p)$

Since it is desired that the pendulum is stabilized at the unstable upright position by means of the twisting sliding-mode control [26], the reference values were taken as $q_{rp} = 0$ and $\dot{q}_{rp} = 0$. The hyperbolic tangent function was also used as the sign function. In this case, the inputs for the SMC can be calculated with TSMC in terms of the passive variables.

$$\ddot{q}_p = Q_1 s + Q_2 \tanh(s) + Q_3\dot{s} + Q_4\tanh(\dot{s})$$

with the given references,

$$\ddot{q}_p = -Q_1 q_p - Q_2 \tanh\left(q_p\right) - Q_3\left(\dot{q}_p\right) - Q_4\tanh\left(\dot{q}_p\right)$$

If we want to control the active independent variables of the system, the same procedure is repeated for the active variables.

$q_{ra} = \left[\theta_{2r}\ s_{5r}\right]^T$: the reference inputs

$q_a = [\theta_2\ s_5]^T$: the instantaneous measured input values.

In that case, the sliding surfaces can be defined as.

$s = (q_{ra} - q_a)$ and $\dot{s} = (\dot{q}_{ra} - \dot{q}_a)$

In order to control the inputs of the mechanism (active independent variables), the references are considered as q_{rp} and $\dot{q}_{rp}$.

$$\ddot{q}_a = K_{a1}s + K_{a2}\tanh(s) + K_{a3}\dot{s} + K_{a4}\tanh(\dot{s})$$
$$\ddot{q}_a = -K_{a1}(q_{ra} - q_a) - K_{a2}\tanh(q_{ra} - q_a) - K_{a3}(\dot{q}_{ra} - \dot{q}_a) - K_{a4}\tanh(\dot{q}_{ra} - \dot{q}_a)$$

As a result, (15) was used to control the pendulum angles while (13) was applied for the control law of the actuation mechanism. In the simulations, the coefficients used in the control input of the SMC for both passive case and active case are selected by trial and error as follows.

$Q_1 = \text{diag}[100\ \ 100], Q_2 = \text{diag}[6\ \ 6], Q_3 = \text{diag}[50\ \ 50], Q_4 = \text{diag}[0.4\ \ 0.2]$, $K_{a1} = \text{diag}[17.5\ \ 17.5]$, $K_{a2} = \text{diag}[4.2\ \ 4.2]$, $K_{a3} = \text{diag}[15\ \ 15]$, $K_{a1} = \text{diag}[0.9\ \ 0.9]$.

3.2 Linear quadratic Gaussian control

LQG control is one of the most fundamental optimal control problems of control theory. The problem is related to the control of uncertain linear systems subjected to a second-order cost function. These systems have a missing state information and additional disturbance of white Gaussian noise. At the end of the solution of this problem, a unique dynamic feedback control law which can be easily calculated and implemented is obtained. The LQG controller is a combination of the linear quadratic regulator (LQR) and the Kalman filter that is a linear quadratic estimator (LQE). The method also holds good for linear time-invariant systems as well as linear time-variant ones. In order to use this method, the system must first be linearized on a specified point.

Linearization of the model and obtaining the state space: Let's $x = \left[q\ \ \dot{q}\right]^{\mathrm{T}}$ be the state variables of the system. So, the nonlinear equation of (8) can be written as follows.

$$\frac{\mathrm{d}}{\mathrm{d}t}\begin{bmatrix} q \\ \dot{q} \end{bmatrix} = f(x,\tau) = \begin{bmatrix} \dot{q} \\ M(q)^{-1}\left[\tau - C(q,\dot{q})\right] \end{bmatrix} \tag{16}$$

When the system is at the equilibrium position, the inputs and state variables can be specified as in matrix form like $\tau_e = \left[0\ 0\right]^T$ and $x_e = \left[0\ \ \frac{\pi}{2}\ \ 0\ 0\ 0\ 0\ 0\ 0\right]$.

The nonlinear system can be represented in state space form.

$$\begin{aligned} \dot{x} &= Ax + Bu + w_d \\ y &= Cx + w_n \end{aligned} \tag{17}$$

where A, B and C matrices can be calculated at the given equilibrium position by using (8) with $A = \left.\frac{\partial f(x,\tau)}{\partial x}\right|_{\tau=\tau_e, x=x_e}$ $B = \left.\frac{\partial f(x,\tau)}{\partial \tau}\right|_{\tau=\tau_e, x=x_e}$ $C = \left.\frac{\partial f(Outputs)}{\partial x}\right|_{\tau=\tau_e, x=x_e}$. w_d is the system noises represented by a white noise with a mean of zero on actuators and an impulsive input at specified times to the pendulum, w_n is the observation noise represented with a mean of zero. The following matrices are obtained numerically for the equilibrium points and constant parameters given in Table 1.

$$A = \begin{bmatrix} 0 & 0 & 0 & 0 & 1 & 0 & 0 & 0 \\ 0 & 0 & 0 & 0 & 0 & 1 & 0 & 0 \\ 0 & 0 & 0 & 0 & 0 & 0 & 1 & 0 \\ 0 & 0 & 0 & 0 & 0 & 0 & 0 & 1 \\ 0 & 0 & 4.17 & -14.81 & 0 & 0 & 0 & 0 \\ 0 & 0 & -0.62 & -0.29 & 0 & 0 & 0 & 0 \\ 0 & 0 & 48.56 & -1.88 & 0 & 0 & 0 & 0 \\ 0 & 0 & -1.88 & 52.68 & 0 & 0 & 0 & 0 \end{bmatrix}, \quad B = \begin{bmatrix} 0 & 0 \\ 0 & 0 \\ 0 & 0 \\ 0 & 0 \\ 202.82 & 3.98 \\ 3.98 & 1.75 \\ 25.8 & -3.82 \\ -91.44 & -1.80 \end{bmatrix},$$

$$C = \begin{bmatrix} 1 & 0 & 0 & 0 & 0 & 0 & 0 & 0 \\ 0 & 1 & 0 & 0 & 0 & 0 & 0 & 0 \\ 0 & 0 & 1 & 0 & 0 & 0 & 0 & 0 \\ 0 & 0 & 0 & 1 & 0 & 0 & 0 & 0 \end{bmatrix}.$$

LQG Design: In order to be able to apply LQG control to a linear system which generally appears as in the diagram given in Fig. 5, LQR controller design should be preliminarily done. At first, the linear system seen in (17) has been subjected to a quadratic cost function given in (18) and then the states that optimize this cost function have been carried out by solving the Riccati differential equation.

$$J_{LQR} = \int_0^\infty \left(x^T Q x + u^T R u\right)\mathrm{d}t \tag{18}$$

In this cost function, x represents the states, u inputs, Q and R the weight matrices. These weight matrices can be written

Table 1 The constant parameters of the inverted pendulum system

Dimensions (m)	Masses (kg)	Inertias (kgm^2)
$L_1 = 0.3$	$m_2 = 0.08783$	$I_{2z} = 32013.27 \times 10^{-9}$
$L_2 = 0.1$	$m_3 = 0.22421$	$I_{3z} = 2875910.82 \times 10^{-9}$
$L_3 = 0.35$	$m_4 = 0.14778$	$I_{4z} = 183814.49 \times 10^{-9}$
$L_4 = 0.2$	$m_5 = 0.29133$	$I_{\mathrm{Penx}} = 1293944.167 \times 10^{-9}$
$L_{\mathrm{Pen}} = 0.4$	$m_{\mathrm{Pen}} = 0.057$	$I_{\mathrm{Peny}} = 1310147.04 \times 10^{-9}$
		$I_{\mathrm{Penz}} = 23001.97 \times 10^{-9}$

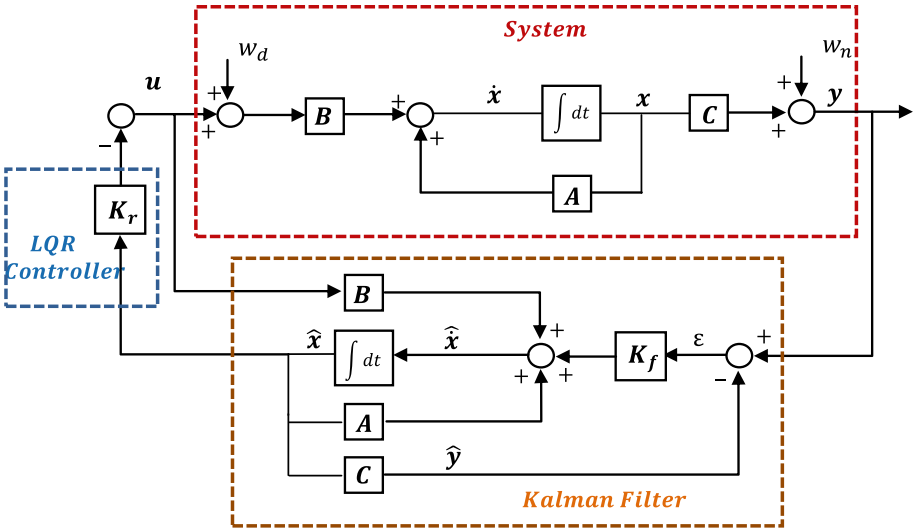

Fig. 5 The block diagram of LQG controller

depending on the desired behavior of the system. The Riccati matrix equation and its solution were defined in (19–21).

$$A^T L + LA - LBR^{-1}B^T L + Q = 0 \tag{19}$$

$$K_r = R^{-1}B^T L \tag{20}$$

$$u = -K_r x \tag{21}$$

The solution of (19) is L and it makes the system stable. (20) gives the static gain constant, K_r, while (21) generates the inputs that will optimize the states. Meanwhile, Q and R matrices which are positive semi-definite and positive definite, respectively, were arbitrarily chosen as follows for the inverted pendulum system.

$$Q = \begin{bmatrix} 0&0&0&0&1&0&0&0\\ 0&0&0&0&0&1&0&0\\ 0&0&0&0&0&0&1&0\\ 0&0&0&0&0&0&0&1\\ 0&0&0&0&1&0&0&0\\ 0&0&0&0&0&1&0&0\\ 0&0&0&0&0&0&\rho&0\\ 0&0&0&0&0&0&0&\rho \end{bmatrix}, \quad \rho = 0.75 \quad R = \begin{bmatrix} \gamma & 0 \\ 0 & \gamma \end{bmatrix}, \quad \gamma = 0.015$$

These values were substituted into (20) to obtain the static gain constant K_r.

$$K_r = \begin{bmatrix} 2.27 & 0 & 0 & 1.44 & 21.71 & 0 & 0 & 7.07 \\ 0 & -6.83 & 1.43 & 0 & 0 & -60.07 & 7.07 & 0 \end{bmatrix}$$

State estimator design:

The equations belonging to Kalman filter to estimate the other states by means of the measured states are given below. Here, $\hat{x}$ represents the estimated states, $\hat{y}$ the estimated outputs, ε the error between the measured and estimated outputs and K_f the Kalman gain considered as an updater between the measured and estimated outputs.

$$\dot{\hat{x}} = A\hat{x} + Bu + K_f\varepsilon \tag{22}$$

$$\hat{y} = C\hat{x} \tag{23}$$

$$\varepsilon = y - \hat{y} \tag{24}$$

In a similar manner to the LQR controller design with Kalman filter, the error (ε) is optimized by subjecting to a scalar cost function defined in (25). So as to do this, it is necessary to solve again a Riccati differential equation.

$$J_{KF} = \lim_{n\to\infty} E\Big(\big[y - \hat{y}\big]^T \big[y - \hat{y}\big] \Big) \tag{25}$$

$$AP + PA^T - PC^T {R_{se}}^{-1} CP + Q_{se} = 0 \tag{26}$$

$$K_f = PB^T {R_{se}}^{-1} \tag{27}$$

In the cost function given in (25), y represents the real output values while $\hat{y}$ stands for the estimated output values. In order to solve the Riccati equation, we need again the weight matrices. In our system, these matrices were defined as Q_{se} and R_{se} the same as the LQR weight matrices. Kalman filter gain (K_f) was obtained by getting P from the above equations.

Combination of LQR and state estimator (LQE):

If (17) and (22) are combined and rearranged, then the LQG controller will be achieved via the combination of LQR and LQE (Kalman filter).

$$\left.\begin{aligned} \dot{x} &= Ax + Bu + w_d \\ y &= Cx + w_n \end{aligned}\right\} \text{Linear system} \tag{28}$$

$$\left.\begin{aligned}\dot{\hat{x}} &= A\hat{x} + Bu + K_f\varepsilon\\ \hat{y} &= C\hat{x}\\ \varepsilon &= y - \hat{y} = Cx + w_n - C\hat{x}\end{aligned}\right\}\ \text{Estimator} \tag{29}$$

Arranging these two equations for the whole system, it can be said that the controller represents a dynamic system by itself. The expression in matrix form is given as follows.

$$\begin{bmatrix}\dot{x}\\ \dot{\hat{x}}\end{bmatrix} = \begin{bmatrix}A & -BK_r\\ K_fC & A - BK_r - K_fC\end{bmatrix}\begin{bmatrix}x\\ \hat{x}\end{bmatrix} + \begin{bmatrix}I & 0\\ 0 & K_f\end{bmatrix}\begin{bmatrix}w_d\\ y\end{bmatrix} \tag{30}$$

This equation was used to control the inverted pendulum system with the LQG on the different conditions.

4 Results

In this section, the previously designed SOSMC and LQG controllers were simulated by using MATLAB over the dynamic model and the results were comparatively evaluated according to the controller performances which are robustness, response time and stability. An external disturbance of white Gaussian noise was added on the system in all simulations. One of the most important studies to assess the designed controllers was to examine the behavior of the system for the impulse disturbances applied to the spatial inverted pendulum. Also, these simulations are important to show the success of the actuation mechanism designed for the control of the pendulum in this study. The simulations started from the equilibrium position and were lasting for 1 second. The impulsive input was applied for 0.001 seconds at 0.2 second of the simulation. The value of the disturbing impulse was gradually increased until the controllers failed to bring the pendulum to the equilibrium position. The responses to these inputs for both controllers are given in Figs. 6 and 7 for two angles of the pendulum.

As shown in the figure, the SOSMC could be imposed to an impulsive torque up to 7.5 mNm (mN:millli-Newton) and the LQG controller up to 10 mNm as a disturbance. In addition, the maximum disturbance of 7.5 mNm brought about approximately the deviation angle of 4° on α while a maximum deviation of 5.5° was observed for LQG controller. In Fig. 6, a similar aspect is seen on the β angle. When using SOSMC, a deviation of 2.1° on the β angle is observed at the impulsive torque of 3.5 mNm, while the LQG controller possesses an angle of 6°. The first outcome here is that the LQG controller is more robust than the SOSMC for the disturbing impulses. However, when stabilizing time is evaluated, the SOSMC performs the stabilization process of the pendulum faster than the LQG controller. In the meanwhile, these results with the absorbed deviations of up to 6°on both angles seem to be closely consistent with the results of an

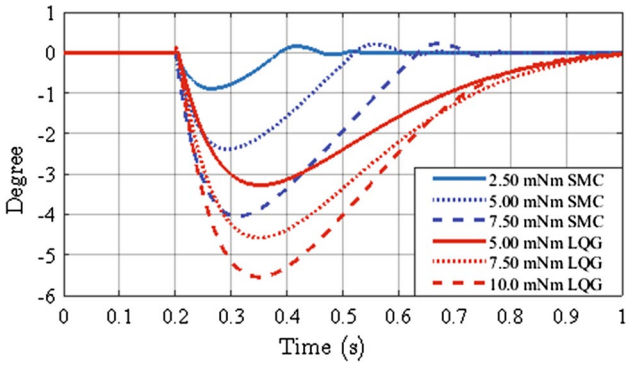

Fig. 6 The time responses to the disturbing impulsive inputs for α

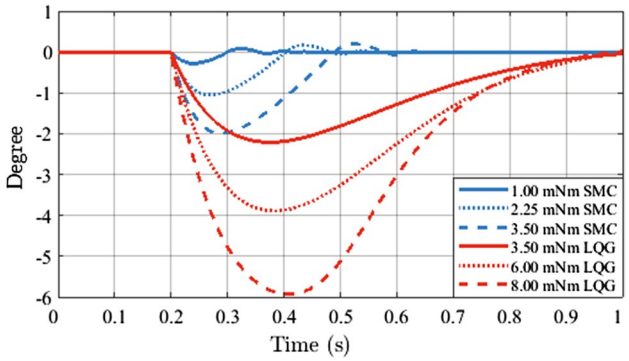

Fig. 7 The time responses to the disturbing impulsive inputs for β

experimental study which is balancing of a spatial inverted pendulum actuated via a 5R mechanism [12]. In this study, some disturbances were applied to the spatial pendulum by knocking and both deflection angles of about 5° were absorbed in a short time.

Figure 8 shows the reactions of the SOSMC and LQG controller to the different initial angels α and β. Examining the graph, it can be seen that the SOSMC can balance the initial angle of α up to a maximum of 8° and the initial angle of β up to a minimum of −8°. In the LQG controller, it is seen that these angles is 11° for α and −11° for β. Thus, the LQG controller is more robust for the responses to the initial angles.

Another important aspect is that stabilizing the inverted pendulum and keeping it in equilibrium for a long period of time. The study on this subject is given in Fig. 9. During the long working period, the disturbance impulsive inputs to the pendulum were applied at the 15th and 30th seconds of the simulation. The outcomes show that the LQG controller can keep the pendulum in equilibrium for long period of time because it was linearized about the specified point on which the dexterity of the workspace is very high. In addition, in this study, as previously expressed, a white noise

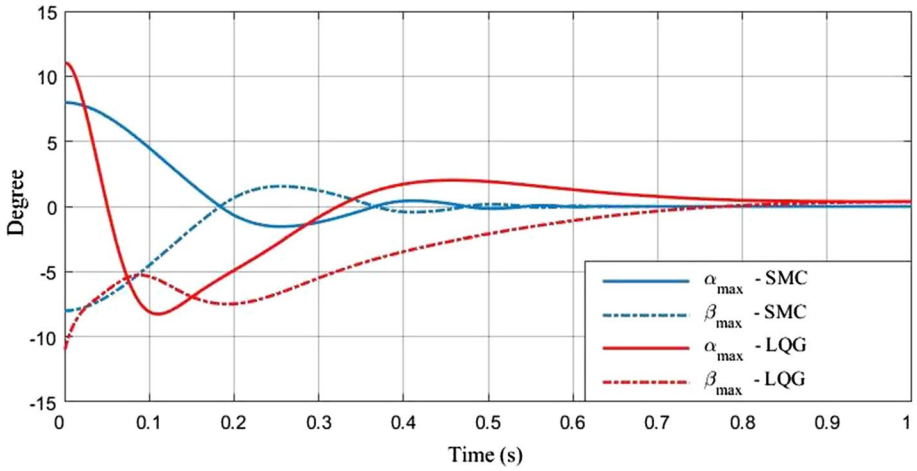

Fig. 8 The responses to the initial angles

with specified amplitudes was applied to the inputs. With this study, the SOSMC can compensate the noise band of ±0.05 Nm to the rotational actuator and ±0.05 N to the linear actuator, while the LQG controller can tolerate the noise bands of ±1.0 Nm and ±1.0 N respectively.

By using the LQG method, a sample animation on the balancing of the spatial inverted pendulum is given by using in Online Resource 1 [27].

Another study on the spatial inverted pendulum was the investigation of the system response to the change of pendulum length. All parameters were kept constant and simulations were performed by taking the length of L/2, L, 2L, and 3L. In this study, using only the LQG controller, the maximum impulsive disturbing values were investigated for the different lengths of the pendulum. The results are given in Fig. 10.

It is observed that the tolerable value of the impulsive input increases as the length of the pendulum increases. For example, the impulsive torque in the direction of alpha is 0.108 mNm for L / 2, 0.146 mNm for L, 0.196 mNm for 2L and 0.295 mNm for 3L. On the other hand, the maximum angle corresponding to these tolerable impulse torques are 16° , 9° , 5° and 3.5° for L / 2, L, 2L and 3L, respectively. This shows that the pendulum with the shorter lengths is stabilized even for larger deflection angles. This indicates physically that the pendulum with smaller inertia can be brought to equilibrium with less effort.

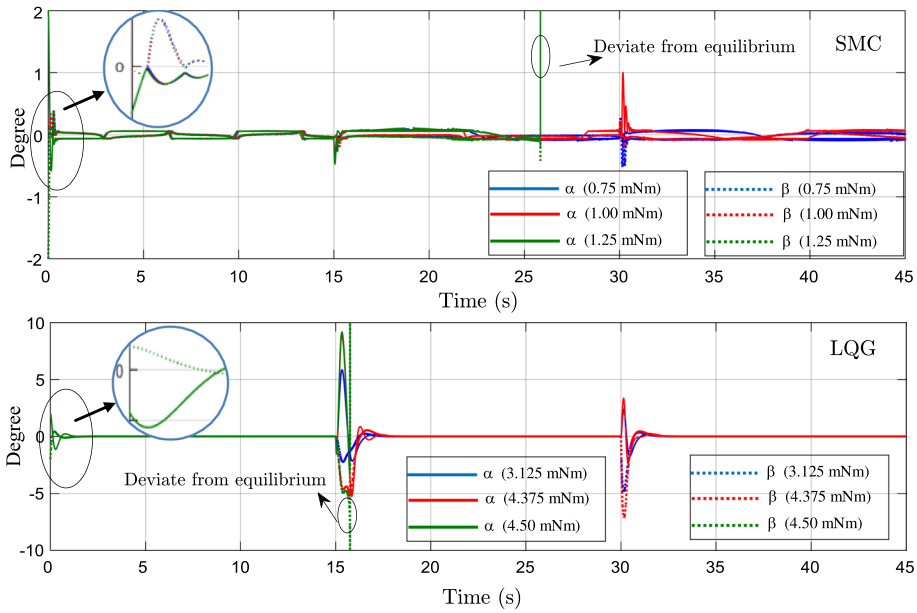

Fig. 9 Keeping the pendulum in equilibrium for a long period of time

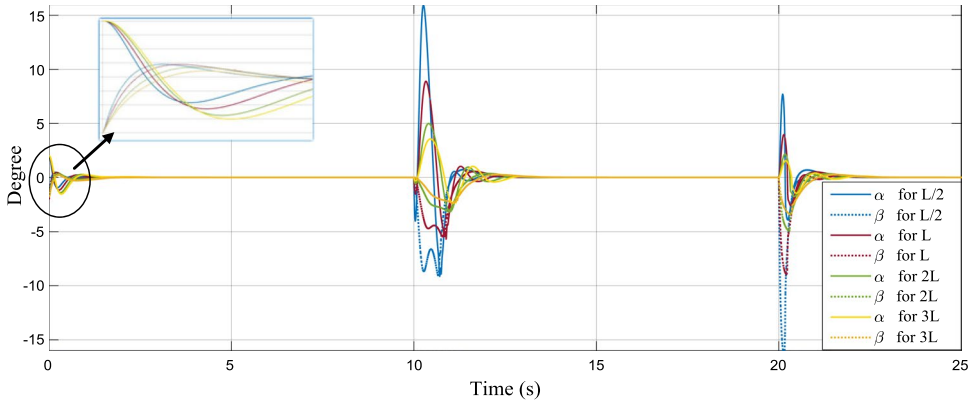

Fig. 10 The responses to the change of pendulum length

5 Discussion and conclusion

In this paper, the kinematic and dynamic modeling of a spatial inverted pendulum system was presented. This system is nonlinear and requires a fast response for the stabilizing control of the pendulum in upright position. An actuation mechanism with PRRRR planar structure in this pendulum system has not been used in literature so far. The dimensional design of the mechanism has been achieved successfully based on an optimization with genetic algorithm. According to these design parameters, the dexterity workspace which is determined via the pivot point of the mechanism was presented in this paper to move the platform to the suitable region without blocking over all the operations. In simulations, SOSMC and LQG controller have been used to keep the pendulum in equilibrium. In balancing, the SOSMC is more robust and faster than LQG controller for disturbing effects. However, the LQG controller shows better performance for the initial positions of the pendulum and keeping it in the stable position for a long period of time. For the future work, another paper will be assigned on the setup and real-time controller design of the spatial inverted pendulum.

Appendix

The following relations were obtained from the dynamic analysis and used in the control algorithms. In these expressions, s_{qk} and c_{qk}stand for the abbreviations of sin (q_k) and cos (q_k)respectively.

The Inertial terms:

$$M(q_k) = \begin{bmatrix} \begin{bmatrix} m_{11} & m_{12} \\ m_{21} & m_{22} \end{bmatrix} & \begin{bmatrix} m_{13} & m_{14} \\ m_{23} & m_{24} \end{bmatrix} \\ \begin{bmatrix} m_{31} & m_{32} \\ m_{41} & m_{42} \end{bmatrix} & \begin{bmatrix} m_{33} & m_{34} \\ m_{43} & m_{44} \end{bmatrix} \end{bmatrix} = \begin{bmatrix} M_{aa} & M_{ap} \\ M_{pa} & Mp_p \end{bmatrix}$$

$$\begin{aligned}
m_{11} &= 0.25(4I_{2_z} + 4b_3^2 I_{3_z} + 4b_4^2 I_{4_z} + L_2^2 m_2 + 4L_2^2 m_3 \\
&+ b_3^2 L_3^2 m_3 + b_4^2 L_4^2 m_4 + 4\, b_3 L_2 L_3\, m_3 \mathrm{c}_{(\theta_2-\theta_3)} \\
&+ 4\, b_3^2 (I_{py}\, \mathrm{s}_\alpha^2 + \mathrm{c}_\alpha^2 (I_{pz} \mathrm{c}_\beta^2 + I_{px} \mathrm{s}_\beta^2) \\
&+ m_6 \left((2L_2 \mathrm{c}_{\theta_2} + b_3 \mathrm{c}_{\theta_3} (L_3 + L_p \mathrm{s}_\beta)) + b_3 L_p \mathrm{c}_\beta) \mathrm{s}_\alpha) \mathrm{s}_{\theta 3})\right)^2 \\
&+ (-b_3 L_p \mathrm{c}_\beta \mathrm{c}_{\theta_3} \mathrm{s}\alpha + 2L_2 \mathrm{s}_{\theta_2} + b_3 (L_3 + L_p \mathrm{s}_\beta) \mathrm{s}_{\theta_3}^2))
\end{aligned}$$

$$\begin{aligned}
m_{12} = m_{21} &= 0.0625(4a_4 b_4 (4I_{4_z} + L_4^2 m_4) + a_3 b_3 (16 I_{3_z} \\
&+ 8I_{py} + 3L_p^2 m_6 + 4L_3^2 (m_3 + m_6)) - a_3 b_3 (8I_{py} + L_p^2 m_6) \mathrm{c}_\alpha \\
&+ 2a_3 b_3 \mathrm{c}_\alpha^2 (4(I_{px} + I_{pz}) - (4I_{px} - 4I_{pz} + L_p^2 m_6) \mathrm{c}_{2\beta}) \\
&+ 8b_4 L_4 m_4 \mathrm{c}_{\theta_4} + 8a_3 (L_2\, \mathrm{c}_{(\theta_2-\theta_3)} (L_3\, (m_3 + m_6) + L_p\, m_6\, \mathrm{s}_\beta) \\
&+ L_p\, m_6 (b_3 L_3 \mathrm{s}_\beta - L_2 \mathrm{c}_\beta \mathrm{s}_\alpha \mathrm{s}_{(\theta_2-\theta_3)}))
\end{aligned}$$

$$\begin{aligned}
m_{13} = m_{31} &= 0.25 \mathrm{c}_\alpha \mathrm{c}_\beta (b_3 L_3 L_p m_6 + 2L_2 L_p m_6 \mathrm{c}_{(\theta_2-\theta_3)} \\
&+ b_3 (4I_{px} - 4I_{pz} + L_p^2 m_6) \mathrm{s}_\beta)
\end{aligned}$$

$$\begin{aligned}
m_{14} = m_{41} &= 0.25(\mathrm{s}_\alpha (b_3 (4I_{py} + L_p^2 m_6) + L_p m_6 (b_3 L_3 \\
&+ 2L_2 \mathrm{c}_{(\theta 2-\theta 3)}) \mathrm{s}_\beta - 2L_2 L_p m_6 \mathrm{c}_\beta s_{(\theta 2-\theta 3)})
\end{aligned}$$

$$\begin{aligned}
m_{22} &= a_3^2\, I_{3_z} + a_4^2 I_{4_z} + 0.25\; a_3^2 L_3^2\, m_3 + \; m_4 \\
&+ a_4^2 L_4^2\, m_4 + m_5 + a_4 L_4\, m_4\, \mathrm{c}_{\theta 4} \\
&+ 0.25\, a_3^2 m_6 (L_p^2 \mathrm{c}_\beta^2 \mathrm{s}_\alpha^2 + (L_3 + L_p\, \mathrm{s}_\beta)^2 \\
&+ a_3^2\, (I_{py} \mathrm{s}_\alpha^2 + \mathrm{c}_\alpha^2 (I_{pz} \mathrm{c}_\beta^2 + I_{px} \mathrm{s}_\beta^2))
\end{aligned}$$

$$m_{23} = m_{32} = -0.25 a_3 \mathrm{c}_\alpha \mathrm{c}_\beta (L_3 L_p m_6 + (4I_{px} - 4I_{pz} + L_p^2 m_6) \mathrm{s}_\beta)$$

$$m_{24} = m_{42} = 0.25 a_3 \mathrm{s}_\alpha (4I_{py} + L_p^2 m_6 + L_3 L_p m_6 \mathrm{s}_\beta)$$

$$m_{33} = 0.125(4(I_{px} + I_{pz}) + L_p^2 m_6 + (4I_{px} - 4I_{pz} + L_p^2 m_6) \mathrm{c}_{2\beta})$$

$$m_{34} = m_{43} = 0$$

$$m_{44} = I_{py} + L_p^2 m_6 / 4$$

The Coriolis, centrifugal and gravity acceleration terms:

$$C(q_k, \dot{q}_k) = \begin{bmatrix} \begin{bmatrix} c_{11} \\ c_{21} \end{bmatrix} \\ \begin{bmatrix} c_{31} \\ c_{41} \end{bmatrix} \end{bmatrix} = \begin{bmatrix} C_a \\ C_p \end{bmatrix},$$

$$
\begin{aligned}
c_{11} &= 0.25(4b_3 I_{3z} k_{c1} + 4b_4 I_{4z} k_{c2} + b_4 k_{c2} L_4^2 m_4 \\
&- 4b_3 (\mathrm{c}_{\theta 3}\dot{\alpha} - \mathrm{c}_{\alpha}\mathrm{s}_{\theta 3}\dot{\beta})((-(I_{px} - I_{pz})\mathrm{c}_{\beta}\mathrm{c}_{\theta 3}\mathrm{s}_{\alpha}\mathrm{s}_{\beta} \\
&+ I_{pz}\mathrm{c}_{\beta}^2\mathrm{s}_{\alpha}^2\mathrm{s}_{\theta 3} + (I_{py}\mathrm{c}_{\alpha}^2 + I_{px}\mathrm{s}_{\alpha}^2\mathrm{s}_{\beta}^2)\,\mathrm{s}_{\theta 3})\dot{\alpha} \\
&+ \mathrm{c}_{\alpha}(I_{px}\mathrm{c}_{\beta}^2\mathrm{c}_{\theta 3} + I_{pz}\mathrm{c}_{\theta 3}\mathrm{s}_{\beta}^2 - (I_{px} - I_{pz})\,\mathrm{c}_{\beta}\,\mathrm{s}_{\alpha}\mathrm{s}_{\beta}\mathrm{s}_{\theta 3})\dot{\beta}) \\
&+ 4b_3 (\mathrm{s}_{\theta 3}\dot{\alpha} + \mathrm{c}_{\alpha}\mathrm{c}_{\theta 3}\dot{\beta})\,((I_{py}\,\mathrm{c}_{\beta}^2\mathrm{c}_{\theta 3} \\
&+ \mathrm{s}_{\alpha}(I_{pz}\mathrm{c}_{\beta}^2\,\mathrm{c}_{\theta 3}\mathrm{s}_{\alpha} + I_{px}\mathrm{c}_{\theta 3}\mathrm{s}_{\alpha}\mathrm{s}_{\beta}^2 + (I_{px} - I_{pz})\,\mathrm{c}_{\beta}\mathrm{s}_{\beta}\,\mathrm{s}_{\theta 3}))\,\dot{\alpha} \\
&- \mathrm{c}_{\alpha}\,((I_{px} - I_{pz})\,\mathrm{c}_{\beta}\mathrm{c}_{\theta 3}\mathrm{s}_{\alpha}\mathrm{s}_{\beta} + I_{px}\mathrm{c}_{\beta}^2\,\mathrm{s}_{\theta 3} + I_{pz}\,\mathrm{s}_{\beta}^2\mathrm{s}_{\theta 3})\,\dot{\beta}) \\
&+ 4\,b_3\,(I_{py}\,\mathrm{s}_{\alpha}^2 + \mathrm{c}_{\alpha}^2(I_{pz}\mathrm{c}_{\beta}^2 + I_{px}\,\mathrm{s}_{\beta}^2))\;(k_{c1} + \mathrm{c}_{\alpha}\dot{\alpha}\dot{\beta}) \\
&+ L_3 m_3(k_{c1}(b_3 L_3 + 2L_2\mathrm{c}_{(\theta 2-\theta 3)}) + 2a_3^2 L_2\mathrm{s}_{(\theta 2-\theta 3)}\dot{s}_5^2 \\
&+ 4\,a_3\,b_3 L_2\mathrm{s}_{(\theta 2-\theta 3)}\,\dot{s}_5\,\dot{\theta}_2 + 2(-1 + b_3)\,b_3 L_2\,\mathrm{s}_{(\theta 2-\theta 3)}\dot{\theta}_2^2) \\
&+ 4b_3\,\mathrm{c}_{\alpha}(\mathrm{c}_{\theta 3}\mathrm{s}_{\alpha}(I_{py} - I_{pz}\mathrm{c}_{\beta}^2 - I_{px}\mathrm{s}_{\beta}^2) \\
&+ \;(-I_{px} + I_{pz})\,\mathrm{c}_{\beta}\mathrm{s}_{\beta}\mathrm{s}_{\theta 3})\,(-\mathrm{c}_{\alpha}\mathrm{s}_{\theta 3}\,\dot{\beta}\,(a_3\dot{s}_5 \\
&+ b_3\,\dot{\theta}_2) + \mathrm{c}_{\theta 3}\dot{\alpha}(a_3\dot{s}_5 - \mathrm{s}_{\alpha}\dot{\beta} + b_3\,\dot{\theta}_2)) \\
&+ 4b_3\,\mathrm{c}_{\alpha}(-(I_{px} - I_{pz})\mathrm{c}_{\beta}\mathrm{c}_{\theta 3}\mathrm{s}_{\beta} + I_{pz}\mathrm{c}_{\beta}^2\mathrm{s}_{\alpha}\mathrm{s}_{\theta 3} \\
&+ \mathrm{s}_{\alpha}(-I_{py} + I_{px}\mathrm{s}_{\beta}^2)\mathrm{s}_{\theta 3})(-\mathrm{c}_{\alpha}\mathrm{c}_{\theta 3}\dot{\beta}\,(a_3\,\dot{s}_5 + b_3\,\dot{\theta}_2) \\
&- \mathrm{s}_{\theta 3}\dot{\alpha}\,(a_3\dot{s}_5 - \mathrm{s}_{\alpha}\dot{\beta} + b_3\,\dot{\theta}_2)) + m_6\;((b_3 L_p\mathrm{c}_{\beta}\mathrm{c}_{\theta 3}\mathrm{s}_{\alpha} \\
&- 2\,L_2\mathrm{s}_{\theta 2} - b_3\,(L_3 + L_p\,\mathrm{s}_{\beta})\,\mathrm{s}_{\theta 3})\,(k_{c1}L_p\mathrm{c}_{\beta}\mathrm{c}_{\theta 3}\mathrm{s}_{\alpha} - k_{c1}(L_3 \\
&+ L_p\mathrm{s}_{\beta})\mathrm{s}_{\theta 3} - L_p\mathrm{c}_{\beta}\mathrm{s}_{\alpha}\mathrm{s}_{\theta 3}\,\dot{\alpha}^2 \\
&- 2L_p\mathrm{c}_{\alpha}\mathrm{s}_{\beta}\mathrm{s}_{\theta 3}\,\dot{\alpha}\dot{\beta} - L_p\mathrm{c}_{\theta 3}\,\mathrm{s}_{\beta}\,\dot{\beta}^2 - L_p\mathrm{c}_{\beta}\mathrm{s}_{\alpha}\mathrm{s}_{\theta 3}\dot{\beta}^2 \\
&- 2L_2\mathrm{c}_{\theta 2}\dot{\theta}_2^2 + 2L_p\mathrm{c}_{\alpha}\mathrm{c}_{\beta}\mathrm{c}_{\theta 3}\dot{\alpha}(a_3\dot{s}_5 + b_3\,\dot{\theta}_2) \\
&- 2L_p\,\mathrm{c}_{\theta 3}\,\mathrm{s}_{\alpha}\mathrm{s}_{\beta}\dot{\beta}(a_3\dot{s}_5 + b_3\dot{\theta}_2) - 2L_p\,\mathrm{c}_{\beta}\,\mathrm{s}_{\theta 3}\dot{\beta}(a_3\,\dot{s}_5 \\
&+ b_3\,\dot{\theta}_2) - \mathrm{c}_{\theta 3}(L_3 + L_p\mathrm{s}_{\beta})\,(a_3\,\dot{s}_5 + b_3\,\dot{\theta}_2^2 - L_p\,\mathrm{c}_{\beta}\,\mathrm{s}_{\alpha}\mathrm{s}_{\theta 3}\,(a_3\dot{s}_5 \\
&+ b_3\,\dot{\theta}_2^2) + (2\,L_2\;\mathrm{c}_{\theta 2} + b_3\,\mathrm{c}_{\theta 3}\,(L_3 + L_p\,\mathrm{s}_{\beta}) \\
&+ \;\; b_3 L_p\,\mathrm{c}_{\beta}\,\mathrm{s}_{\alpha}\mathrm{s}_{\theta 3}\;\;(k_{c1}\mathrm{c}_{\theta 3}\,(L_3 + L_p\,\mathrm{s}_{\beta}) + \;k_{c1}L_p\mathrm{c}_{\beta}\,\mathrm{s}_{\alpha}\mathrm{s}_{\theta 3} \\
&+ L_p\,\mathrm{c}_{\beta}\,\mathrm{c}_{\theta 3}\,\mathrm{s}_{\alpha}\dot{\alpha}^2 + 2L_p\,\mathrm{c}_{\alpha}\mathrm{c}_{\theta 3}\mathrm{s}_{\beta}\dot{\alpha}\dot{\beta}) \\
&+ L_p\mathrm{c}_{\beta}\mathrm{c}_{\theta 3}\,\mathrm{s}_{\alpha}\dot{\beta}^2 - L_p\mathrm{s}_{\beta}\mathrm{s}_{\theta 3}\dot{\beta}^2 \\
&- 2L_2\mathrm{s}_{\theta 2}\dot{\theta}_2^2 + 2L_p\,\mathrm{c}_{\alpha}\mathrm{c}_{\beta}\mathrm{s}_{\theta 3}\dot{\alpha}(a_3\dot{s}_5 \\
&+ b_3\,\dot{\theta}_2) + 2L_p\mathrm{c}_{\beta}\mathrm{c}_{\theta 3}\dot{\beta}(a_3\dot{s}_5 + b_3\dot{\theta}_2) \\
&- 2L_p\,\mathrm{s}_{\alpha}\mathrm{s}_{\beta}\mathrm{s}_{\theta 3}\,\dot{\beta}\,(a_3\dot{s}_5 + b_3\,\dot{\theta}_2) \\
&+ L_p\mathrm{c}_{\beta}\,\mathrm{c}_{\theta 3}\mathrm{s}_{\alpha}(a_3\dot{s}_5 + b_3\;\dot{\theta}_2^2 - (L_3 + L_p\mathrm{s}_{\beta})\mathrm{s}_{\theta 3}(a_3\dot{s}_5 \\
&+ b_3\;\dot{\theta}_2^2)) + 2b_3\,\mathrm{c}_{\alpha}((-I_{px} + 2I_{py} - I_{pz} \\
&+ (I_{px} - I_{pz})\mathrm{c}_{\beta})\,\mathrm{s}_{\alpha}\,\dot{\alpha} + (I_{px} - I_{pz})\,\mathrm{c}_{\alpha}\mathrm{s}_{2\beta}\dot{\beta})(\mathrm{s}_{\alpha}\dot{\beta} + \dot{\theta}_3)))
\end{aligned}
$$

$$
\begin{aligned}
c_{12} &= a_3 I_{3z} k_{c1} + a_4 I_{4z} k_{c2} - a_3(\mathrm{c}_{\theta 3}\dot{\alpha} - \mathrm{c}_{\alpha}\mathrm{s}_{\theta 3}\dot{\beta}) \\
&((-(I_{px} - I_{pz})\mathrm{c}_{\beta}\mathrm{c}_{\theta 3}\mathrm{s}_{\alpha}\mathrm{s}_{\beta} + I_{pz}\mathrm{c}_{\beta}^2\mathrm{s}_{\alpha}^2\mathrm{s}_{\theta 3} \\
&+ (I_{py}\mathrm{c}_{\alpha}^2 + I_{px}\,\mathrm{s}_{\alpha}^2\mathrm{s}_{\beta}^2)\mathrm{s}_{\theta 3})\dot{\alpha} + \mathrm{c}_{\alpha}(I_{px}\,\mathrm{c}_{\beta}^2\mathrm{c}_{\theta 3} \\
&+ I_{pz}\,\mathrm{c}_{\theta 3}\mathrm{s}_{\beta}^2 - (I_{px} - I_{pz})\mathrm{c}_{\beta}\mathrm{s}_{\alpha}\mathrm{s}_{\beta}\mathrm{s}_{\theta 3})\,\dot{\beta}) \\
&+ a_3\;(\mathrm{s}_{\theta 3}\dot{\alpha} + \;\mathrm{c}_{\alpha}\mathrm{c}_{\theta 3}\,\dot{\beta})((I_{py}\mathrm{c}_{\alpha}^2\mathrm{c}_{\theta 3} \\
&+ \;\mathrm{s}_{\alpha}(I_{pz}\,\mathrm{c}_{\beta}^2\,\mathrm{c}_{\theta 3}\mathrm{s}_{\alpha} + I_{px}\,\mathrm{c}_{\theta 3}\mathrm{s}_{\alpha}\mathrm{s}_{\beta}^2 + (I_{px} \\
&- I_{pz})\mathrm{c}_{\beta}\mathrm{s}_{\beta}\mathrm{s}_{\theta 3}))\dot{\alpha} - \mathrm{c}_{\alpha}((I_{px} - I_{pz})\mathrm{c}_{\beta}\mathrm{c}_{\theta 3}\,\mathrm{s}_{\alpha}\mathrm{s}_{\beta} \\
&+ I_{px}\,\mathrm{c}_{\beta}^2\,\mathrm{s}_{\theta 3} + I_{pz}\;\mathrm{s}_{\beta}^2\mathrm{s}_{\theta 3})\dot{\beta}) + a_3\,(I_{py}\mathrm{s}_{\alpha}^2 \\
&+ \mathrm{c}_{\alpha}^2(I_{pz}\mathrm{c}_{\beta}^2 + I_{px}\mathrm{s}_{\beta}^2)(k_{c1} + \mathrm{c}_{\alpha}\dot{\alpha}\dot{\beta}) \\
&+ 0.25\,a_3\;L_3\,m_3(k_{c1}L_3 - 2L_2\,\mathrm{s}_{(\theta 2-\theta 3)}\dot{\theta}_2^2) \\
&+ 0.25L_4 m_4(a_4 k_{c2}L_4 + 2k_{c2}\mathrm{c}_{\theta 4} - 2a_4^2\mathrm{s}_{\theta 4}\dot{s}_5^2 \\
&- 4a_4 b_4\mathrm{s}_{\theta 4}\dot{s}_5\dot{\theta}_2 - 2b_4^2\mathrm{s}_{\theta 4}\dot{\theta}_2^2) + a_3\,\mathrm{c}_{\alpha}(\mathrm{c}_{\theta 3}\mathrm{s}_{\alpha} \\
&(I_{py} - I_{pz}\mathrm{c}_{\beta}^2 - I_{px}\mathrm{s}_{\beta}^2) + (-I_{px} + I_{pz}) \\
&\mathrm{c}_{\beta}\mathrm{s}_{\beta}\mathrm{s}_{\theta 3})\,(-\mathrm{c}_{\alpha}\mathrm{s}_{\theta 3}\,\dot{\beta}(a_3\dot{s}_5 + b_3\dot{\theta}_2) \\
&+ \mathrm{c}_{\theta 3}\dot{\alpha}(a_3\dot{s}_5 - \mathrm{s}_{\alpha}\dot{\beta} + b_3\,\dot{\theta}_2)) \\
&+ a_3\mathrm{c}_{\alpha}(-(I_{px} - I_{pz})\,\mathrm{c}_{\beta}\mathrm{c}_{\theta 3}\,\mathrm{s}_{\beta} + I_{pz}\,\mathrm{c}_{\beta}^2\mathrm{s}_{\alpha} \\
&\mathrm{s}_{\theta 3} + \mathrm{s}_{\alpha}(-I_{py} + I_{px}\,\mathrm{s}_{\beta}^2)\mathrm{s}_{\theta 3})\,(-\mathrm{c}_{\alpha}\mathrm{c}_{\theta 3}\;\dot{\beta}(a_3\dot{s}_5 \\
&+ b_3\,\dot{\theta}_2) - \mathrm{s}_{\theta 3}\dot{\alpha}(a_3\dot{s}_5 - \mathrm{s}_{\alpha}\,\dot{\beta} + b_3\,\dot{\theta}_2)) \\
&+ 0,0625a_3 m_6(4k_{c1}L_3^2 + 3\,k_{c1}L_p^2 \\
&- k_{c1}\,L_p^2\mathrm{c}_{\alpha}^2 - k_{c1}\,L_p^2\mathrm{c}_{\beta}^2 - k_{c1}\,L_p^2\mathrm{c}_{\alpha}^2\mathrm{c}_{\beta}^2 \\
&+ k_{c1}L_p^2\mathrm{s}_{\alpha}^2 + k_{c1}Lp^2\mathrm{c}_{\beta}^2\mathrm{s}_{\alpha}^2 + 8\,k_{c1}L_3 L_p\,\mathrm{s}_{\beta} \\
&+ k_{c1}L_p^2\mathrm{s}_{\beta}^2 + k_{c1}\,L_p^2\mathrm{c}_{\alpha}^2\mathrm{s}_{\beta}^2 - k_{c1}\,L_p^2\mathrm{s}_{\alpha}^2\mathrm{s}_{\beta}^2 \\
&+ 4L_p\,\mathrm{c}_{\beta}\mathrm{s}_{\alpha}\;(L_3 + L_p\,\mathrm{s}_{\beta})\,\dot{\alpha}^2 \\
&+ 4L_3\,L_p\,\mathrm{c}_{\beta}\,\mathrm{s}_{\alpha}\dot{\beta}^2 + 4\,a_3\,L_p\mathrm{c}_{\beta}\dot{s}_5(L_p \\
&\mathrm{c}_{\beta}\,\mathrm{s}_{2\alpha}\dot{\alpha} + \;2(\,L_3 + L_p\mathrm{c}_{\alpha}^2\mathrm{s}_{\beta})\,\dot{\beta}) \\
&+ 8\,b_3 L_3 L_p\mathrm{c}_{\beta}\dot{\beta}\dot{\theta}_2 + 2\,b_3 L_p^2\,\mathrm{s}_{2\beta}\,\dot{\beta}\,\dot{\theta}_2 \\
&+ 2b_3\,L_p^2\mathrm{c}_{\alpha}^2\mathrm{s}_{2\beta}\dot{\beta}\dot{\theta}_2 - 2b_3\,L_p^2\,\mathrm{s}_{\alpha}^2\mathrm{s}_{2\beta}\dot{\beta}\dot{\theta}_2 \\
&- 8L_2 L_p\,\mathrm{c}_{\beta}\mathrm{c}_{\theta 2}\mathrm{c}_{\theta 3}\,\mathrm{s}_{\alpha}\dot{\theta}_2^2 \;- 8L_2 L_3\,\mathrm{c}_{\theta 3}\mathrm{s}_{\theta 2}\dot{\theta}_2^2 \\
&- 8\,L_2 L_p\,\mathrm{c}_{\beta}\,\mathrm{s}_{\alpha}\mathrm{s}_{\theta 2}\,\mathrm{s}_{\theta 3}\,\dot{\theta}_2^2 + 2L_p\mathrm{c}_{\alpha}\,\dot{\alpha}\,(4\,\mathrm{s}_{\beta}(L_3 \\
&+ L_p\mathrm{s}_{\beta})\,\dot{\beta} + 4b_3\,L_p\mathrm{c}_{\beta}^2\mathrm{s}_{\alpha}\dot{\theta}_2)) \\
&- 8L_2 L_p\;\mathrm{c}_{\theta 3}\,\mathrm{s}_{\beta}\mathrm{s}_{\theta 2}\dot{\theta}_2^2 \;+ 8\,L_2\,L_3\mathrm{c}_{\theta 2}\mathrm{s}_{\theta 3}\,\dot{\theta}_2^2 \\
&+ 8L_2\,L_p\mathrm{c}_{\theta 2}\mathrm{s}_{\beta})\,\mathrm{s}_{\theta 3}\,\dot{\theta}_2^2 \;+ 0.5\;a_3\,\mathrm{c}_{\alpha} \\
&((-I_{px} + 2I_{py} - I_{pz} + (I_{px} - I_{pz})\mathrm{c}_{2\beta})\mathrm{s}_{\alpha}\dot{\alpha} \\
&+ (I_{px} - I_{pz})\mathrm{c}_{\alpha}\mathrm{s}_{2\beta}\dot{\beta})(\mathrm{s}_{\alpha}\dot{\beta} + \dot{\theta}_3)
\end{aligned}
$$

$$
\begin{aligned}
c_{13} &= 0.125k_{c1}L_p^2m_6\mathrm{c}_\alpha\mathrm{s}_{2\beta} - a_3^2L_p^2m_6\mathrm{c}_\beta^2\mathrm{s}_{2\alpha}\dot{s}_5^2 \\
&- 4b_3I_{px}\mathrm{c}_\alpha\dot{\beta}\dot{\theta}_2 - (-2k_{c1}L_3L_pm_6\mathrm{c}_\alpha\mathrm{c}_\beta \\
&+ 4gL_p\,m_p\mathrm{c}_\beta\mathrm{s}_\alpha - 4I_{px}\,k_{c1}\mathrm{c}_\alpha\mathrm{s}_{2\beta} + 4I_{pz}k_{c1}\mathrm{c}_\alpha\mathrm{s}_{2\beta} \\
&- 4b_3I_{pz}\mathrm{c}_\alpha\dot{\beta}\dot{\theta}_2 - 2b_3L_p^2m_6\,\mathrm{c}_\alpha\,\dot{\beta}\dot{\theta}_2 \\
&- 4b_3I_{px}\mathrm{c}_\alpha\mathrm{c}_\beta^2\dot{\beta}\dot{\theta}_2 + 4b_3I_{pz}\,\mathrm{c}_\alpha\,\mathrm{c}_\beta^2\dot{\beta}\,\dot{\theta}_2 \\
&- 2\,b_3L_p^2\,m_6\,\mathrm{c}_\alpha\mathrm{c}_\beta^2\,\dot{\beta}\dot{\theta}_2 + 4b_3\,I_{px}\mathrm{c}_\alpha\mathrm{s}_\beta^2\dot{\beta}\dot{\theta}_2 \\
&- 4b_3I_{pz}\mathrm{c}_\alpha\mathrm{s}_\beta^2\dot{\beta}\dot{\theta}_2 + 2b_3L_p^2m_6\mathrm{c}_\alpha\mathrm{s}_\beta^2\dot{\beta}\,\dot{\theta}_2 \\
&- b_3^2L_p^2m_6\mathrm{c}_\alpha\mathrm{s}_\alpha\dot{\theta}_2^2 - b_3^2L_p^2m_6\mathrm{c}_\alpha\mathrm{c}_\beta^2\mathrm{s}_\alpha\dot{\theta}_2^2 \\
&+ b_3^2L_p^2\,m_6\,\mathrm{c}_\alpha\mathrm{s}_\alpha\mathrm{s}_\beta^2\dot{\theta}_2^2 \\
&+ 4L_2L_p\,m_6\mathrm{c}_\alpha\mathrm{c}_\beta\mathrm{c}_{\theta3}\mathrm{s}_{\theta2}\dot{\theta}_2^2 \\
&- 4L_2L_pm_6\mathrm{c}_\alpha\mathrm{c}_\beta\mathrm{c}_{\theta2}\,\mathrm{s}_{\theta3}\,\dot{\theta}_2^2 + a_3\,\dot{s}_5 \\
&(4\,(I_{px} - I_{pz})\,\mathrm{s}_\alpha\mathrm{s}_{2\beta}\dot{\alpha} - 2\,\mathrm{c}_\alpha((2I_{px} + 2I_{pz} + L_p^2m_6 \\
&+ (2I_{px} - 2I_{pz} + L_p^2\,m_6)\,\mathrm{c}_{2\beta}\dot{\beta} + 2b_3\,L_p^2\,m_6\,\mathrm{c}_\beta^2 \\
&\mathrm{s}_\alpha\dot{\theta}_2)) - 2\mathrm{s}_{2\beta}\dot{\alpha}((4I_{px} - 4I_{pz} + L_p^2m_6)\,\dot{\beta} \\
&- 2(I_{px} - I_{pz})\,\mathrm{s}_\alpha(b_3\dot{\theta}_2 - \dot{\theta}_3)) + 4I_{px}\,\mathrm{c}_\alpha\dot{\beta}\dot{\theta}_3 - 8I_{py} \\
&\mathrm{c}_\alpha\dot{\beta}\,\dot{\theta}_3 + 4\,I_{pz}\mathrm{c}_\alpha\,\dot{\beta}\dot{\theta}_3 - 4I_{px}\,\mathrm{c}_\alpha\,\mathrm{c}_\beta^2\dot{\beta}\,\dot{\theta}_3 \\
&+ 4I_{pz}\,\mathrm{c}_\alpha\,\mathrm{c}_\beta^2\dot{\beta}\dot{\theta}_3 + 4I_{px}\,\mathrm{c}_\alpha\mathrm{s}_\beta^2\dot{\beta}\,\dot{\theta}_3 \\
&- 4I_{pz}\,\mathrm{c}_\alpha\,\mathrm{s}_\beta^2\dot{\beta}\dot{\theta}_3 + 2I_{px}\,\mathrm{s}_{2\alpha}\,\dot{\theta}_3^2 \\
&- 4I_{py}\,\mathrm{s}_{2\alpha}\dot{\theta}_3^2 + 2I_{pz}\,\mathrm{s}_{2\alpha}\dot{\theta}_3^2 - 2I_{px} \\
&\mathrm{c}_\beta^2\mathrm{s}_{2\alpha}\,\dot{\theta}_3^2 + 2I_{pz}\,\mathrm{c}_\beta^2\mathrm{s}_{2\alpha}\dot{\theta}_3^2 \\
&+ 2I_{px}\,\mathrm{s}_{2\alpha}\mathrm{s}_\beta^2\dot{\theta}_3^2 - 2I_{pz}\mathrm{s}_{2\alpha}\mathrm{s}_\beta^2\,\dot{\theta}_3^2\,) \\
c_{14} &= 0.125(8I_{py}k_{c1}\mathrm{s}_\alpha + 2k_{c1}L_p^2m_6\mathrm{s}_\alpha \\
&+ 4gL_pm_p\mathrm{c}_\alpha\mathrm{s}_\beta + 2k_{c1}L_3L_pm_6\mathrm{s}_\alpha\mathrm{s}_\beta \\
&- 2a_3^2L_pm_6\mathrm{c}_\beta(L_3 + L_p\mathrm{c}_\alpha^2\mathrm{s}_\beta)\dot{s}_5^2 \\
&+ (4I_{px} - 4I_{pz} + L_p^2m_6)\,\mathrm{s}_{2\beta}\,\dot{\alpha}^2 \\
&- 2b_3^2L_3L_p\,m_6\,\mathrm{c}_\beta\dot{\theta}_2^2 - 4L_2L_pm_6\mathrm{c}_\beta\,\mathrm{c}_{\theta2}\mathrm{c}_{\theta3}\dot{\theta}_2^2 \\
&- b_3^2L_p^2m_6\mathrm{c}_\beta\mathrm{s}_\beta\dot{\theta}_2^2 - b_3^2L_p^2m_6\mathrm{c}_\alpha^2\mathrm{c}_\beta\mathrm{s}_\beta\dot{\theta}_2^2 \\
&+ b_3^2L_p^2m_6\mathrm{c}_\beta\mathrm{s}_\alpha^2\mathrm{s}_\beta\dot{\theta}_2^2 - 4L_2L_pm_6\mathrm{c}_{\theta3}\mathrm{s}_\alpha\mathrm{s}_\beta\mathrm{s}_{\theta2}\dot{\theta}_2^2 \\
&+ 4L_2L_pm_6\mathrm{c}_{\theta2}\mathrm{s}_\alpha\mathrm{s}_\beta\mathrm{s}_{\theta3}\dot{\theta}_2^2 - 4L_2L_p\,m_6\mathrm{c}_\beta\mathrm{s}_{\theta2}\mathrm{s}_{\theta3}\dot{\theta}_2^2\,a_3\dot{s}_5 \\
&+ (2\,\mathrm{c}_\alpha(4I_{py} + Lp^2\,m_6 + L_p^2m_6\,\mathrm{c}_{2\beta})\,\dot{\alpha} \\
&- 4\,b_3L_p\,m_6\,\mathrm{c}_\beta(L_3 + L_p\,\mathrm{c}_\alpha^2\mathrm{s}_\beta)\,\dot{\theta}_2) - 2I_{px}\mathrm{s}_{2\beta}\,\dot{\theta}_3^2 \\
&+ 2I_{pz}\mathrm{s}_{2\beta}\dot{\theta}_3^2 - 2I_{px}\mathrm{c}_\alpha^2\mathrm{s}_{2\beta}\dot{\theta}_3^2 + 2I_{pz}\,\mathrm{c}_\alpha^2 \\
&\mathrm{s}_{2\beta}\,\dot{\theta}_3^2 + 2I_{px}\,\mathrm{s}_\alpha^2\mathrm{s}_{2\beta}\dot{\theta}_3^2 \\
&- 2I_{pz}\,\mathrm{s}_\alpha^2\mathrm{s}_{2\beta}\dot{\theta}_3^2 + 2\mathrm{c}_\alpha\dot{\alpha}(b_3(4I_{py} + L_p^2m_6 \\
&+ L_p^2m_6\mathrm{c}_{2\beta})\dot{\theta}_2 + 4(I_{px} - I_{pz})\mathrm{c}_{2\beta}\dot{\theta}_3))
\end{aligned}
$$

The acceleration coefficients:

$$
\begin{aligned}
k_{a1} &= -(L_2\mathrm{Csc}_{(\theta_3-\theta_4)}\mathrm{s}_{(\theta_2-\theta_4)})/L_3 \\
1\,k_{b1} &= -(\mathrm{Csc}_{(\theta_3-\theta_4)}\mathrm{s}_{\theta_4})/L_3 \\
k_{c1} &= -(\mathrm{Csc}_{(\theta3-\theta4)}(L_2\mathrm{c}_{(\theta2-\theta4)}\dot{\theta}_2^2 + L_3\mathrm{c}_{(\theta3-\theta4)}\dot{\theta}_3^2 - L_4\dot{\theta}_4^2))/L_3 \\
k_{a2} &= -(L_2\mathrm{Csc}_{(\theta3-\theta4)}\mathrm{s}_{(\theta2-\theta3)})/L_4 \\
k_{b2} &= -(\mathrm{Csc}_{(\theta3-\theta4)}\mathrm{s}_{\theta4})/L_4 \\
k_{c2} &= -(\mathrm{Csc}_{(\theta3-\theta4)}(-L_2\mathrm{c}_{(\theta2-\theta3)}\dot{\theta}_2^2 - L_3\dot{\theta}_3^2 + L_4\mathrm{c}_{(\theta3-\theta4)}\dot{\theta}_4^2))/L_4
\end{aligned}
$$

The velocity coefficients:

$$
\begin{aligned}
a_3 &= -(\mathrm{Csc}_{(\theta3-\theta4)}\mathrm{s}_{\theta4})/L_3 \\
b_3 &= -(L_2\mathrm{Csc}_{(\theta3-\theta4)}\mathrm{s}_{(\theta2-\theta4)})/L_3 \\
a_4 &= -(\mathrm{Csc}_{(\theta3-\theta4)}\mathrm{s}_{\theta3})/L_4 \\
b_4 &= -(L_2\mathrm{Csc}_{(\theta3-\theta4)}\mathrm{s}_{(\theta2-\theta3)})/L_4
\end{aligned}
$$

The actuator terms:

$$
\tau\left(q_k, \dot{q}_k\right) = \begin{bmatrix} \begin{bmatrix} \tau_2 \\ f_5 \end{bmatrix} \\ \begin{bmatrix} 0 \\ 0 \end{bmatrix} \end{bmatrix} = \begin{bmatrix} \tau \\ 0 \end{bmatrix}
$$

References

1. Liu C, Ning J, Chen Q (2018) Dynamic walking control of humanoid robots combining linear inverted pendulum mode with parameter optimization. Int J Adv Robot Syst 15(1):1–15. https://doi.org/10.1177/1729881417749672
2. Wilson J, Charest M, Dubay R (2016) Non-linear model predictive control schemes with application on a 2 link vertical robot manipulator. Robot Comput-Integr Manuf 41:23–30. https://doi.org/10.1016/j.rcim.2016.02.003
3. Semenov ME, Meleshenko PA, Solovyov AM, Semenov AM (2015) Structural nonlinear dynamics and diagnosis: hysteretic nonlinearity in inverted pendulum problem. Springer, Cham, pp 463–506
4. Wang JJ, Liu DL, Wang BJ (2014) Research on one type of saturated nonlinear stabilization control method of X–Z inverted pendulum. Acta Autom Sin 39(1):92–96. https://doi.org/10.1016/S1874-1029(13)60011-7
5. Roose AI, Yahya S, Al-Rizzo H (2017) Fuzzy-logic control of an inverted pendulum on a cart. Comput Electr Eng 61:1339–1351. https://doi.org/10.1016/j.compeleceng.2017.05.016
6. De Almeida R, Nyandoro O (2017) Swing-up control of the Acrobot using noncollocated partial feedback linearisation: an algorithmic approach. Pattern recognition association of south africa and robotics and mechatronics (PRASA-RobMech), IEEE, pp 98–103. https://doi.org/10.1109/RoboMech.2017.8261130.
7. Huynh XD, Khanh D, Huynh L, Dat VD (2017) Application of fuzzy algorithm in optimizing hierarchical sliding mode control for pendubot System. Robot Manag 22(2):8–12
8. Seifried R (2014) Dynamics of underactuated multibody systems. Springer, Berlin
9. Mohan V, Rani A, Singh V (2017) Robust adaptive fuzzy controller applied to double inverted pendulum. J Intell Fuzzy Syst 32(5):3669–3687. https://doi.org/10.3233/JIFS-169301
10. Al-Janan DH, Chang HC, Chen YP, Liu TK (2017) Optimizing the double inverted pendulum's performance via the uniform neuro multiobjective genetic algorithm. Int J Autom Comput 14(6):686–695. https://doi.org/10.1007/s11633-017-1069-8
11. Ishii C, Nishitani Y, Hashimoto H (2009) Modelling and robust stabilisation of a closed-link 2-dof inverted pendulum with gain scheduled control. Int J Model Identif Control 6(4):320–332. https://doi.org/10.1504/IJMIC.2009.024739

12. Soto I, Campa R (2015) Modelling and control of a spherical inverted pendulum on a five-bar mechanism. Int J Adv Robot Syst 12(7):95. https://doi.org/10.5772/60027
13. Chopra V, Singla SK, Dewan L (2015) Stabilization of an X–Y inverted pendulum using adaptive gain scheduling PID controllers. J Eng Res 3(2):59–78. https://doi.org/10.7603/s40632-015-0014-7
14. Viet TD, Doan PT, Giang H, Kim HK, Kim SB (2012) Control of a 2-DOF omnidirectional mobile inverted pendulum. J Mech Sci Technol 26(9):2921–2928. https://doi.org/10.1007/s12206-012-0710-2
15. Chiu CH, Wang WJ (2018) Implementation of a ball inverted pendulum with omnidirectional moving ability using a robust fuzzy control strategy. ISA Trans 86:287–298. https://doi.org/10.1016/j.isatra.2018.10.012
16. Albouy X, Praly L (2000) On the use of dynamic invariants and forwarding for swinging up a spherical inverted pendulum. In: Proceedings of the 39th IEEE conference on decision and control. December, Sydney, pp 1667–1672
17. Chung CY (2002) Balancing of an inverted pendulum with a kinematically redundant robot. Int J Gen Syst 31(1):1–15. https://doi.org/10.1080/03081070290007995
18. Wai RJ, Chang LJ (2006) Adaptive stabilizing and tracking control for a nonlinear inverted-pendulum system via sliding-mode technique. IEEE Trans Ind Electron 53(2):674–692. https://doi.org/10.1109/TIE.2006.870680
19. Wai RJ, Chang LJ (2006b) Stabilizing and tracking control of nonlinear dual-axis inverted-pendulum system using fuzzy neural network. IEEE Trans Fuzzy Syst 14(1):145–168. https://doi.org/10.1109/TFUZZ.2005.859305
20. Wai RJ, Lee JD, Chang LJ (2003) Development of adaptive sliding-mode control for nonlinear dual-axis inverted-pendulum system. IEEE/ASME Int Conf Adv Intell Mechatron Kobe, Japan 2003:815–820
21. Peng Y, Chiu C, Tsai W, Chou M (2009) Design of an omnidirectional spherical robot: using fuzzy control. In: Proceedings of the international multiconference of engineers and computer scientists, Hong-Kong, pp 1–5
22. Lauwers, TB, Kantor, GA, Hollis RL (2006) A dynamically stable single-wheeled mobile robot with inverse mouse-ball drive. In: Proceedings—IEEE international conference on robotics and automation, Orlando, USA, pp 2884–2889
23. Tereshko V (2009) Control and identification of chaotic systems by altering their energy. Chaos Solitons Fractals 40(5):2430–2446. https://doi.org/10.1016/j.chaos.2007.10.056
24. Avanço RH, Tusset AM, Balthazar JM, Nabarrete A, Navarro HA (2018) On nonlinear dynamics behavior of an electro-mechanical pendulum excited by a nonideal motor and a chaos control taking into account parametric errors. J Braz Soc Mech Sci Eng 40(1):23. https://doi.org/10.1007/s40430-017-0955-x
25. Spong MW (1994) Partial feedback linearization of underactuated mechanical systems. In: Proceedings of IEEE/RSJ international conference on intelligent robots and systems (IROS'94), Munich, Germany, pp 314–321
26. Mahjoub S, Mnif F, Derbel N (2013) Second-order sliding mode control applied to inverted pendulum. Adv Robot Mechatron Circuits. https://doi.org/10.1109/STA.2013.6783142
27. Online Recourse 1 (2020), https://drive.google.com/file/d/1-7DaBv8nYOgy6mnWWYtoHVvPR_511Px8/view?usp = sharing